Polarised Neutron Diffraction Study of Spin Localisation in Nb_6I_{11} *

P. Jane Brown and Kurt R. A. Ziebeck
Institute Max von Laue Paul Langevin, Avenue des Martyrs, 156X–38042 Grenoble Cedex, France
Arndt Simon and Michael Sägebarth
Max-Planck-Institut für Festkörperforschung, Heisenbergstrasse 1, 7000 Stuttgart 80, Federal Republic of Germany

The spin density distribution in single crystals of Nb_6I_{11} in an applied field of 4.6 T has been studied using polarised neutron diffraction at 285 and 40 K. At 285 K each Nb_6I_8 cluster in Nb_6I_{11} carries three unpaired spins whereas at 40 K, below the spin-crossover transition, the cluster carries only one unpaired spin. It has been shown that at 40 K the spin density is not delocalised in the cluster, but can be associated with the bonds formed with just one of the Nb atoms. In the higher temperature phase the spin density is found to be more evenly distributed over the cluster, although the moment on one of the three pairs of equivalent Nb atoms is significantly higher than that on the other two. These results can be understood in terms of earlier molecular orbital calculations.

Transition metal cluster compounds have been a subject of considerable interest over the last 20 years. These compounds are characterised by clusters of metal atoms with distances between them close to those found in the pure metals, the clusters being linked together through non-metal atoms by predominantly covalent bonds. Nb_6I_{11} is one such cluster compound which is of particular interest because of its magnetic properties. The structure and some physical properties of Nb_6I_{11} were investigated more than a decade ago,[1,2] but only fairly recently have developments in the techniques for molecular orbital calculations made it possible to elaborate models which can explain the relationship between its structure and its magnetic properties.

The structure of Nb_6I_{11} is characterised by units of six Nb atoms arranged in an octahedron surrounded by eight iodine atoms in a distorted cube, one over each face of the octahedron. The units are connected by six additional bridging iodine atoms, one opposite each apex and shared between two clusters according to the formula $Nb_6I_8I_{6/2}$.[1] The occurrence of an Nb_6I_8 arrangement is rather surprising, because each cluster only has 19 electrons available for 12 metal–metal bonding orbitals.[2,3] Due to the odd number of electrons in the cluster the compound Nb_6I_{11} is paramagnetic. Locating experimentally the unpaired spin or spins within the cluster should enable the distribution of electrons in the Nb–Nb bonding states to be determined.

The use of polarised neutron scattering to determine the spatial distribution of magnetisation in crystals has been increasingly applied to problems of chemical interest in recent years. The technique is described in ref. 4 and some recent applications in refs. 5—7. In the present paper we describe the use of polarised neutron scattering to locate the magnetisation associated with the unpaired spin in the Nb_6 cluster.

The temperature dependence of the inverse susceptibility of Nb_6I_{11},[8] shown in Figure 1, displays four different regions. In regions II and IV the susceptibility follows Curie-Weiss laws with different effective moments indicating a low-temperature doublet state ($S = \frac{1}{2}$) in region II and a high-temperature quartet state ($S = \frac{3}{2}$) in region IV. At 274 K, the low-temperature limit of region IV, the compound undergoes a structural transition in which the symmetry drops from *Pccn* to $P2_1cn$ and the centre of symmetry of the octahedron is lost.[9]

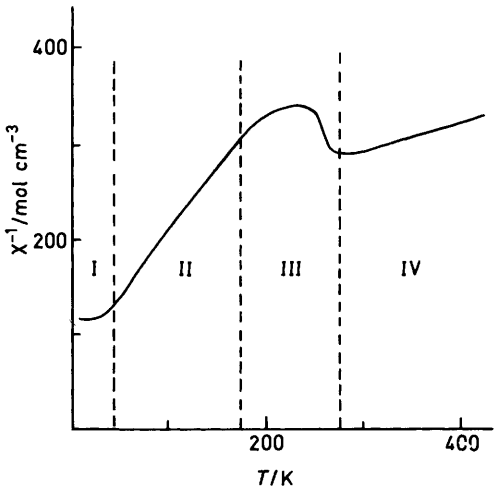

Figure 1. The inverse susceptibility of Nb_6I_{11} (ref. 8)

The change of magnetism through this transition is due to a spin crossover and the behaviour of the susceptibility in regions II, III, and IV is well described in the mean field approximation[10] by a two-state model in which the energy difference between the two states has constant but different values in regions II and IV and varies with temperature and changes sign in region III.[8]

Nohl and Andersen[11] have made a molecular orbital calculation which identifies the lowest unoccupied and highest occupied one-electron levels amongst the five bonding *d* states of highest energy as a function of the distortion of the octahedron which takes place as the temperature is lowered. They found that the effect of increasing distortion is to localise electrons in individual bonds. The geometry of the Nb_6 octahedron at 298 and at 110 K[9] is illustrated in Figure 2 which shows the Nb–Nb interatomic distances. At 298 K the range of Nb–Nb distances is small (274—292 pm) and according to the calculations the upper four of the bonding *d* states are close to one another in energy, and the corresponding electron density is evenly distributed over the octahedron. At 110 K the range of metal–metal distances is greater (268—298 pm) and the molecular orbital model suggests that the states in this case are more widely spaced in energy and localised in

* *Non-S.I. units employed:* Torr ≈ 133 Pa, B.M. ≈ 9.274×10^{-24} J T^{-1}, $\mu_N \approx 5.05 \times 10^{-27}$ J T^{-1}.

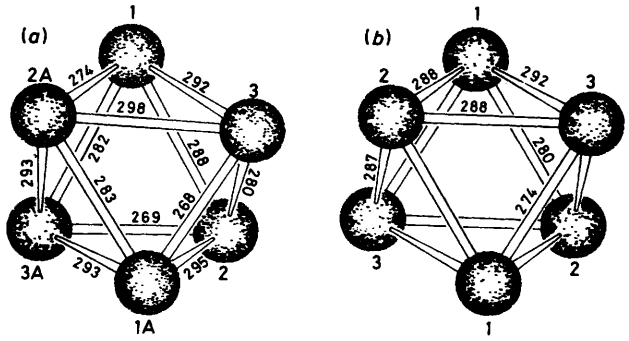

Figure 2. The geometry of the Nb_6 octahedron in Nb_6I_{11} (*a*) at 110 and (*b*) at 298 K (ref. 9). Interatomic distances are given in pm

individual bonds. At low temperatures the states associated with the two shortest bonds [Nb(2)–Nb(3A) 269, Nb(1A)–Nb(3) 268 pm] lie lowest in energy and are doubly occupied; the next lowest state associated with the Nb(1)–Nb(2A) bond (274 pm) is singly occupied and the rest of the states are empty.

The consequences of the molecular orbital model for the spin density distribution are quite dramatic. In the high-temperature phase in which the unpaired electrons are supposed to be distributed over the octahedron, the spin density should be shared evenly amongst the niobium atoms. At low temperatures, on the other hand, the spin density should be confined to just two of the six atoms of the octahedron. The aim of the experiments reported here was to use the polarised neutron technique to study the spin density distribution in both the high- and low-temperature phases of Nb_6I_{11} in order to be able to compare them with these theoretical predictions.

Experimental

Sample Preparation.—The preparation of Nb_6I_{11} previously described[1] was modified to grow large single crystals. A cylindrical niobium crucible (depth 18 cm, volume 125 cm^3) was filled with NaI up to one-third of its depth and covered by a diaphragm of perforated niobium foil carrying Nb_3I_8 (29 g). The crucible was then filled further with NaI (total amount 220 g) and closed by electron beam welding. The starting materials had been purified by distillation (NaI, Merck p.a.; 975 K at 10^{-5} Torr) and chemical transport (Nb_3I_8).[12] For this purpose Nb_3I_8 was prepared from the elements and purified by volatilisation *via* the chemical reaction.[13] $Nb_3I_8(s) + 4\ NbI_5(g) \longrightarrow 7\ NbI_4(g)$, which deposits the compound as large crystals at the colder end of an ampoule in a temperature gradient (1 076—1 025 K). The niobium crucible was enclosed in a jacket of high-strength alloy steel and heated in a temperature gradient of 1 300 (top) to 1 250 K (bottom) in an inclined position. The temperature was lowered at a rate of 1 K h^{-1}. At 970 K the crucible was turned upside down to separate the Naī melt from the Nb_6I_{11} crystals that had collected at the bottom. After opening the cooled crucible under argon, the Nb_6I_{11} crystals were washed with degassed water and dried under vacuum.

Neutron Diffraction Measurements.—The polarised neutron experiments were carried out on the D3 diffractometer at the Institut Laue Langevin (Grenoble), which uses normal beam geometry. The polarisation direction is parallel to the omega axis of the instrument which is also the direction of the magnetic field of 4.6 T applied in the experiment. In both the high- and low-temperature measurements two different crystals were used, mounted so that the field direction was [1,0, $\bar{1}$] for one and [1,$\bar{1}$,0] for the other. For each reflection measured the diffractometer was set so that the peak intensity was received by the detector. With this same orientation the counting rate was measured for neutrons polarised first parallel and then antiparallel to the applied field direction. Under these conditions the ratio R between the two counting rates, commonly known as the 'flipping ratio', is given by equation (1):

$$R = \frac{|N|^2 + |X|^2 + P\cdot(NX^* + N^*X)}{|N|^2 + |X|^2 - Pe\cdot(NX^* + N^*X)} \qquad (1)$$

P is the polarisation of the beam, e the 'flipper efficiency',[14] N is the nuclear structure factor, and X is a vector structure factor which includes all polarisation-dependent contributions to the Bragg scattering.

The susceptibility measurements on Nb_6I_{11}[8] suggest that the moment per Nb_6 cluster induced by the applied field of 4.6 T will be 0.0279 B.M. at 285 K and 0.0634 B.M. at 40 K. These values correspond to maximum magnetic scattering amplitudes of 0.3 and 0.7 fm per unit cell respectively. The corresponding nuclear scattering amplitude is 430 fm giving ratios of magnetic to nuclear scattering of at best 0.0007 and 0.0016 respectively so that the differences in the flipping ratios from unity are *ca.* 0.5% or less. With such a small signal it is not feasible to measure, in a reasonable time, a complete or even an approximately complete set of data from which a spin density map could be constructed.

In the experiments, therefore, measurements were confined to just a few reflections which had reasonably large nuclear structure factors, so that they could be well centred, and for which the magnetic structure factors were calculated to be sensitive to the magnetic model. Good centring is important to avoid spurious contributions to the flipping ratio from the action of the magnetic field in splitting slightly the spin-up and spin-down neutron beams.[15] The optimisation options in the diffractometer control package were used to ensure that all measurements were made on the summits of the reflection profiles. The flipping ratios for the selected reflections were measured from as many equivalents as was possible within the geometric restrictions of the instrument. In all cases the differences between ratios measured for equivalent reflections and between measurements from the two crystals were less than their statistical accuracy. Mean flipping ratios for the set of independent reflections were obtained by averaging together measurements from the two crystals and from all available equivalents, weighting each measurement according to the counting statistics. The standard deviation of the mean was estimated from the differences of individual observations from the mean, or from the counting statistics, whichever gave the greater value.

In order to relate the flipping ratios to the magnetic scattering, knowledge of the nuclear structure factors is required. The parameters for the high-temperature phase at 285 K can be assumed to be the same as those obtained at 298 K in the X-ray structural study;[9] however, the lowest temperature for which X-ray structural parameters are available is 110 K and it was therefore deemed desirable to confirm the structure at 40 K using unpolarised neutron diffraction. For this reason a set of *ca.* 1 300 neutron nuclear structure factors for the [1,0,$\bar{1}$] crystal was measured at 40 K on the D15 single-crystal diffractometer at the Institut Laue Langevin (Grenoble), using normal beam geometry. The measured structure factors were found to be in good agreement with those calculated for the structure at 110 K.[9] Least-squares refinement of the structural parameters revealed no significant evolution between 110 and 40 K. Only one strong low-angle reflection gave any evidence for extinction which it was concluded would give insignificant errors in the magnetic structure factors.

Table 1. Observed and calculated values of γ' at 40 K

					Calculated $10^5\gamma'$		
h	k	l	Schwinger $10^5\gamma'_S$	Observed $10^5\gamma'$	Equal[a]	All on Nb(1), Nb(2A)[b]	Least-squares[c]
0	2	0	0	171(33)	347	274	259
3	3	0	259	67(33)	−24	−54	81
0	4	0	0	287(48)	85	232	258
2	4	0	−2	269(59)	29	189	196
0	6	0	0	88(38)	75	77	73
1	1	1	−14	277(29)	332	334	335
3	2	1	−12	−13(18)	−39	−42	−27
1	5	1	370	174(39)	92	189	221
0	0	2	0	515(29)	410	579	539
3	1	2	63	−141(52)	−93	−121	−155
1	4	2	−62	46(36)	−18	−40	28
1	3	3	−82	102(42)	14	76	100
0	2	4	0	81(27)	106	51	54
1	3	4	111	51(25)	82	78	60
0	2	6	0	73(23)	33	46	27
				χ^2	3.7	2.6	1.4

[a] Models with equally distributed moments. [b] Model with moments equally divided between Nb(1) and Nb(2). [c] Least-squares fit with moments allowed to vary.

Results

When, as in the present case, the nuclear scattering factor $|N|$ is much greater than the spin-dependent scattering factor $|X|$ then a quantity γ' may be defined by equation (2), where $\boldsymbol{p}$ is a unit vector parallel to $\boldsymbol{P}$.

$$2\gamma' = (R - 1)/|\boldsymbol{P}|(1 + e) = \boldsymbol{p}\cdot(N\boldsymbol{X}^* + N^*\boldsymbol{X})/|N|^2 \quad (2)$$

Normally the contribution of magnetic dipole scattering by the outer electrons to $\boldsymbol{X}$ outweighs all other contributions. However in cases such as the present one in which the magnetisation is very small, other small contributions to $\boldsymbol{X}$ must be considered. The most important of these terms are the neutron spin–orbit (Schwinger) scattering and the diamagnetic scattering of the core electrons.

The contribution of Schwinger scattering to $\boldsymbol{X}$ is given by equation (3),[16] where $\boldsymbol{K}$ is the scattering vector, $\boldsymbol{k}$ and $\boldsymbol{k}'$ the

$$\boldsymbol{X}_S = \left(\frac{i}{\boldsymbol{K}^2}\cdot\frac{e^2\gamma m}{mc^2 m_0}\right)(\boldsymbol{k}\cdot\boldsymbol{k}')\Sigma_j[Z_j - f_j(\boldsymbol{K})]\exp(i\boldsymbol{K}\cdot\boldsymbol{r}_j) \quad (3)$$

incident and diffracted wavevectors, m and m_0 the rest masses of electron and neutron, and γ the neutron magnetic moment in nuclear magnetons (μ_N); Z_j is the atomic number of the atom at position $\boldsymbol{r}_j$ in the unit cell and the sum is over all atoms in the unit cell. All other symbols have their usual meanings. The Schwinger scattering is reduced with respect to the magnetic dipole scattering by the factor m/m_0 (0.0005) and has the particularity that it is in quadrature with this scattering as indicated by the factor i in the expression. Because of this phase shift the Schwinger scattering only gives a contribution to the flipping ratio if the nuclear scattering amplitude is complex. In the centrosymmetric phase this can only be due to the imaginary components of the nuclear scattering lengths. For Nb and I these values are 0.01 and 0.006 fm respectively from which it can be shown that the Schwinger contribution to the flipping ratios in the centrosymmetric phase is negligible. However, for the non-centrosymmetric phase the Schwinger scattering adds a term to γ' given by equation (4) for Friedel pairs of reflections

$$2\gamma'_S = (N\boldsymbol{X}_S^* + N^*\boldsymbol{X}_S)/|N|^2 \quad (4)$$

conforming to equations (5) and (6), where S is the Schwinger

$$N(\boldsymbol{K}) = N' + iN'' \text{ and } N(-\boldsymbol{K}) = N' - iN'' \quad (5)$$

$$\boldsymbol{X}_S(\boldsymbol{K}) = iS' + S'' \text{ and } \boldsymbol{X}_S(-\boldsymbol{K}) = iS' - S'' \quad (6)$$

structure factor $-i\boldsymbol{X}_S$. The contribution to R for the two reflections is given by equation (7). Thus the sign of the term

$$2\gamma'_S(\boldsymbol{K}) = (N''S' - S''N')/|N|^2$$
$$\text{and} \quad 2\gamma'_S(-\boldsymbol{K}) = (S''N' - N''S')/|N|^2 \quad (7)$$

added to γ' is opposite for Friedel-paired reflections and should cause them to become inequivalent.

The magnitude of γ'_S was calculated for all the measured reflections and the values are presented in Table 1 alongside the measured values of γ'. It can be seen that for several reflections the predicted size of the Schwinger term is significantly greater than the observed value. In the light of these calculations the equivalence of measurements made on Friedel related reflections was carefully re-examined; no significant differences were found, although in several cases the predicted difference was many times the standard deviation. The fact that such differences are not observed can be understood by recalling that Nb_6I_{11} passes through a structural transition in which the centre of symmetry is lost. If this process is nucleated randomly at many different sites within the crystal then, at low temperatures, the crystal will contain approximately equal volumes of two types of domains: the structure within one type being related to that within the other by inversion. Such domains will make equal and opposite Schwinger contributions to the flipping ratio, thus producing the observed null effect.

The magnetic dipole scattering itself is the sum of a paramagnetic term from the unpaired niobium d electrons and a diamagnetic term from the electrons of the atomic cores. The diamagnetic contribution is given by equation (8)[17] and was

$$\boldsymbol{X}_d = \left(\frac{eH}{hc}\cdot\frac{e^2\gamma}{2mc^2\boldsymbol{K}}\right)\Sigma_j\frac{df_j}{d\boldsymbol{K}}\cdot\exp(i\boldsymbol{K}\cdot\boldsymbol{r}_j) \quad (8)$$

calculated using the exponential approximation to the X-ray scattering factors tabulated by Cromer *et al.*[18] and the relationship (9) in which A_i and B_i are the constants of the

$$\left(\frac{1}{\boldsymbol{K}}\right)\frac{df}{d\boldsymbol{K}} = -\left(\frac{1}{16\pi^2}\right)\Sigma_i A_i B_i\cdot\exp(B_i S^2) \quad (9)$$

expansion and $S = \sin\theta/\lambda$. The calculated diamagnetic contributions were found in all cases to be less than the experimental errors.

Modelling the Spin Density.—Since for neither phase was a complete data set measured, and in addition in the non-centrosymmetric case the magnetic structure factors cannot be deduced directly from the value of γ', the results have been analysed by reference to a simple model. The model assumes that the unpaired spins occupy 4*d*-like states centred on niobium atoms and scatter according to the corresponding spherically symmetric Nb form-factor.[19] The data have been compared with different models in which different proportions of the induced moment are assigned to each of the Nb atoms of the cluster.

For the low-temperature phase the models chosen were one in which the moment was equally distributed over the sites and a second in which it was divided equally between the two Nb

atoms [Nb(1),Nb(2A)] taking part in the bond which was predicted to be spin polarised by Nohl and Andersen.[11] For the centrosymmetric phase the model with equal distribution of moment was compared with one in which the moment was located on just Nb(1) and its centrosymmetrically related partner, and another in which it was confined to just the Nb(2) atoms. Finally for both phases, a least-squares fit of the data to a model, in which the moment on each of the independent Nb atoms was allowed to vary, was carried out subject to the constraint that the sum of all six moments should give the magnetisation. The results of the least-squares fits are given in Table 3 and the calculated values of γ' for the various models are compared with the observations in Tables 1 and 2.

Due to the limited data sets and consequent correlation between the refined parameters, the standard deviations of the parameters obtained in the least-squares fits are probably not good estimates. A better idea of the ability of the data to distinguish between models can be obtained by calculating a goodness of fit (χ^2) using equation (10), where N_o and N_p are the

$$\chi^2 = \frac{[(R_{obs.} - R_{calc.})/\Delta(R_{obs.})]^2}{(N_o - N_p)} \qquad (10)$$

numbers of observations and parameters. On the basis of this criterion the localised model ($\chi^2 = 2.6$) is to be preferred to the delocalised model ($\chi^2 = 3.7$) in the low-temperature phase. In the centrosymmetric phase the model with spin just on the Nb(2) atoms gave a marginally better fit ($\chi^2 = 1.6$) than the delocalised model ($\chi^2 = 1.7$) and a much better fit than that with the moment only on Nb(1) ($\chi^2 = 5.2$). In both phases the moment assignments obtained from least-squares calculations allow a significantly better fit to the data than any of the extreme models ($\chi^2 = 1.2$ and 1.4 for the high- and low-temperature fits respectively).

Discussion

For the low-temperature phase the least-squares fit (see Table 3) suggests that the majority of the moment is associated with the Nb(1) site which is one of those involved in the 'polarised' bond. The other partner in this bond [Nb(2A)] also has significant moment, but there may in addition be some moment on other neighbours of the Nb(1) atom such as Nb(3A). In the centrosymmetric phase the fit suggests that most of the moment is associated with the pair of Nb(2) atoms, the other four atoms in the octahedron each carrying less than one-third of the moment on Nb(2).

Some idea of the spin-density distribution in the two phases can be obtained from the density maps of Figures 3 and 4 in

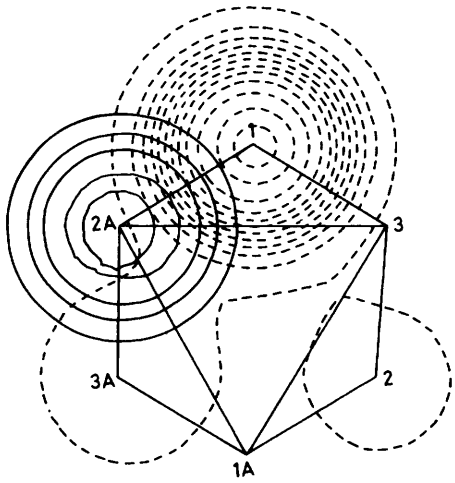

Figure 3. The spin-density distribution in Nb_6I_{11} at 40 K. Solid contours at equal intervals of 5×10^{-4} B.M. Å^{-3} are drawn in the plane of Nb(1A),Nb(2A),Nb(3); dashed contours are the same intervals in the parallel plane through Nb(2). The positions of the Nb atoms are indicated and the Nb_6 octahedron (as seen from above) is outlined

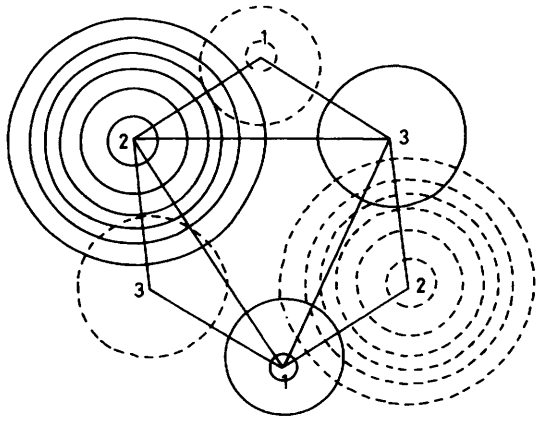

Figure 4. The spin-density distribution in Nb_6I_{11} at 285 K. The contours are drawn and the atom positions marked as in Figure 3 except that the contour intervals are 2.5×10^{-4} B.M. Å^{-3}

Table 2. Observed and calculated values of γ' at 285 K

				Calculated $10^5\gamma'$			
h	k	l	Observed $10^5\gamma'$	Equal[a]	All on Nb(1)[b]	All on Nb(2)[c]	Least-squares[d]
0	2	0	554(194)	570	249	729	643
1	5	0	224(107)	142	20	262	204
3	5	0	156(102)	107	19	110	103
1	1	1	480(93)	544	580	498	519
4	1	1	144(105)	83	21	36	53
1	5	1	374(168)	−94	−262	−12	−56
0	0	2	495(186)	430	825	466	472
3	0	2	−179(181)	114	129	−200	−64
3	1	2	141(77)	−61	−223	39	−13
3	3	2	−67(49)	−60	−253	73	5
4	3	2	−99(71)	−48	−45	−126	−92
2	4	3	−24(143)	−77	−114	15	−27
0	2	4	−240(84)	−117	84	−131	−114
0	3	4	275(80)	138	177	237	197
			χ^2	1.7	5.2	1.6	1.2

[a] Model with equally distributed moments. [b] Model with all moment on Nb(1). [c] Model with all moment on Nb(2). [d] Least-squares fit with moments allowed to vary.

Table 3. The fraction of the total aligned moment found on each of the Nb sites in Nb_6I_{11} at 40 and at 285 K by least-squares fit to the observed values of γ'

Atom	40 K	285 K
Nb(1)	0.58(5)	0.08(9)
Nb(1A)	−0.03(5)	
Nb(2)	0.07(5)	0.35(9)
Nb(2A)	0.23(6)	
Nb(3)	0.05(6)	0.07(9)
Nb(3A)	0.10(6)	

which the spin density corresponding to the models obtained from the least-squares fits is illustrated.

Our measurements are broadly in agreement with the prediction of Nohl and Andersen [11] that the unpaired spin in the low-temperature phase of Nb_6I_{11} is localised within the octahedron rather than distributed equally over it. The unpaired spin appears to be partly, but not totally localised in the Nb(1)–Nb(2A) bond which is that associated with the singly occupied state in the molecular orbital model. The observation of some moment on the Nb(3A) atom which makes the second shortest bond with Nb(1) may indicate that the energy separation between the states associated with the Nb(1)–Nb(2A) and Nb(1)–Nb(3A) bonds is low enough that the higher state is still partially occupied at 40 K.

For the high-temperature phase it may be significant that the two shortest bonds (274 pm) and two longest bonds (292 pm) are between Nb(1) and Nb(3) atoms (Figure 2). Assuming that even at 285 K the low-lying states are associated with short bonds and higher energy ones with long bonds then the low-lying doubly occupied state in the calculation of Nohl and Andersen [11] should be associated with the Nb(1) and Nb(3) atoms. The intermediate bonds which should be singly occupied all involve Nb(2) atoms which may account for the moment being predominantly on this pair of atoms.

References

1 A. Simon. H. G. v. Schnering, and H. Schaefer, *Z. Anorg. Allg. Chem.*, 1967, **355**, 295.
2 F. A. Cotton and T. E. Haas, *Inorg. Chem.*, 1964, **3**, 10.
3 O. K. Andersen, W. Klose, and H. Nohl, *Phys. Rev. B*, 1978, **17**, 1209.
4 P. J. Brown, J. B. Forsyth, and R. Mason, *Philos. Trans. R. Soc. London B*, 1980, **290**, 481.
5 P. Day, *J. Phys.*, 1982, **C-7**, 341.
6 B. N. Figgis, J. B. Forsyth, R. Mason, and P. A. Reynolds, *Chem. Phys. Lett.*, 1985, **115**, 454.
7 G. H. Lander, P. J. Brown, M. R. Spirlet, J. Rebizant, B. Kanellakopulos, and R. Klenze, *J. Chem. Phys.*, 1985, **83**, 5988.
8 J. J. Finley, R. E. Camley, E. E. Vogel, V. Zevin, and E. Gmelin, *Phys. Rev. B*, 1981, **24**, 1322.
9 H. Imoto and A. Simon, *Inorg. Chem.*, 1982, **21**, 308.
10 C. Kittel, 'Introduction to Solid State Physics,' 6th edn., Wiley, New York, 1986.
11 H. Nohl and O. K. Andersen, Proc. Conf. on Transition Metals, Leeds I.O.P. Conf. Ser., 1980, vol. 55, p. 61.
12 H. Schäfer, 'Chemische Transportreaktionen,' Verlag Chemie, Weinheim, 1962.
13 A. Simon and H. G. v. Schnering, *J. Less-Common Met.*, 1966, **11**, 31.
14 P. J. Brown and J. B. Forsyth, *Br. J. Appl. Phys.*, 1964, **15**, 1529.
15 R. M. Moon, W. C. Koehler, and C. H. Shull, *Nucl. Instrum. Meth.*, 1975, **129**, 515.
16 C. G. Shull, *Phys. Rev. Lett.*, 1963, **10**, 297.
17 C. Stassis, *Phys. Rev. Lett.*, 1970, **24**, 1415.
18 D. T. Cromer, A. C. Larsen, and J. T. Waber, *Acta Crystallogr.*, 1964, **17**, 1044.
19 E. Clementi and C. Roetti, *At. Data Nucl. Data Tables*, 1974, **14**, 177.

Received 17*th November* 1986; *Paper* 6/2212